Cholangiolocellular Carcinoma With "Ductal Plate Malformation" Pattern May Be Characterized by ARID1A Genetic Alterations

Motoko Sasaki, MD, PhD, Yasunori Sato, MD, PhD,* and Yasuni Nakanuma, MD, PhD*†*

汇报人：贾旭春

Cholangiolocellular carcinoma (CLC)

- 由小胆道来源的管状癌细胞组成
- 类似胆管反应的细胞构成
- 替代生长模式
- 腔内缺乏黏蛋白产生
- 可与胆管癌（ Cholangiocarcinoma CCA、肝细胞癌（HCC）及混合型肝细胞癌-胆管癌（cHCC-CCA）共存

CLC

04版WHO

- 胆管癌（ CCA）亚型（胆管细胞型）

10版WHO

- 混合型肝细胞癌-胆管癌（cHCC-CCA）亚型（ cHCC-CCA伴干细胞特征，胆管细胞型）

- 排列成腺管状、条索状、相互融合---鹿角样生长方式
- 埋于纤维间质中
- 肿瘤细胞小，核浆比高、核深染、卵圆形
- 重演赫令氏管或胆小管发生
- 轻度不典型性
- 无黏液分泌
- 表达CK19、KIT、NCAM、EpCAM
- 周边可见HCC样和/或CCA样区域
- 肿瘤条索与非肿瘤肝细胞索连续

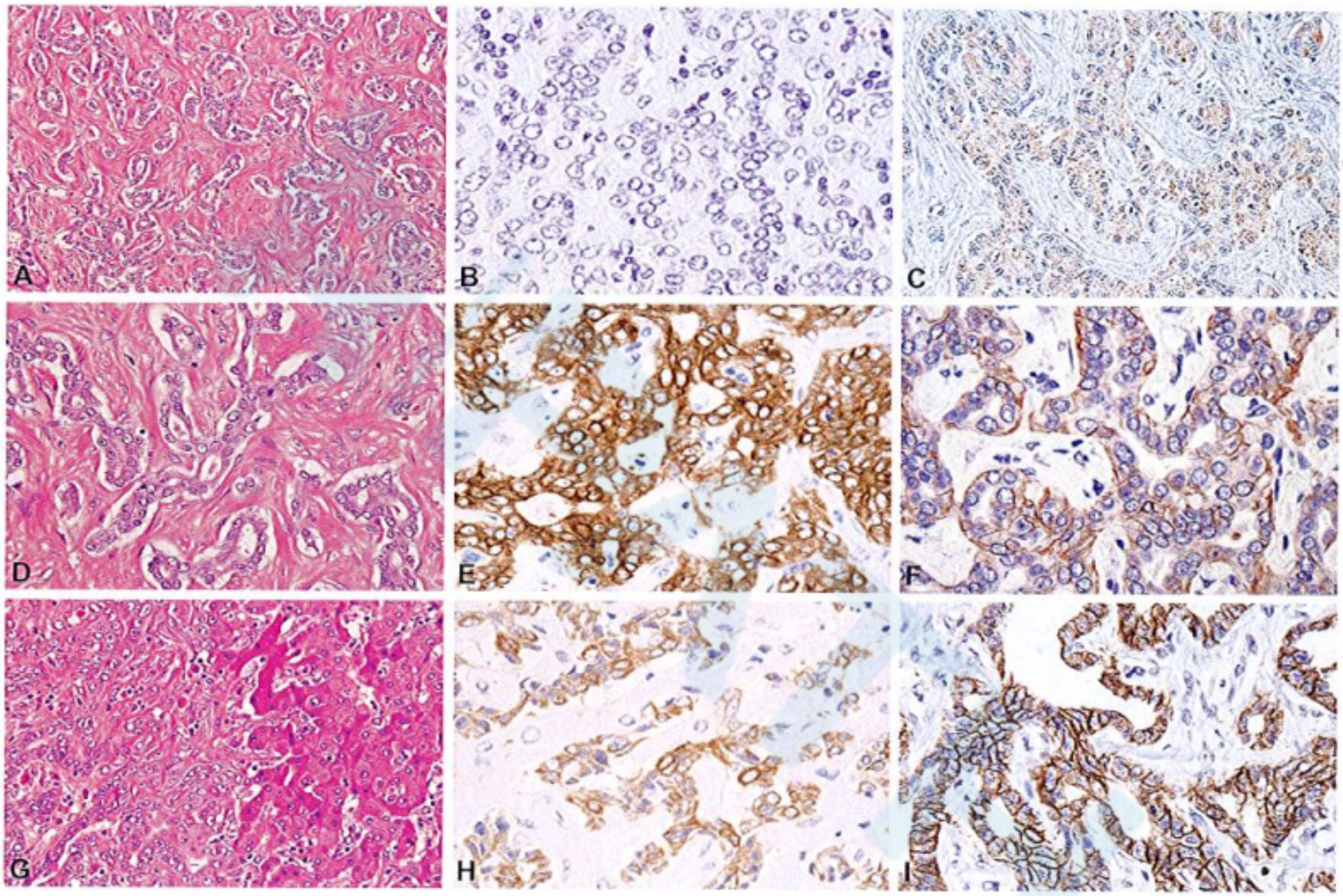

图 10.60 混合型肝细胞癌 - 胆管细胞癌伴干细胞特征，胆管细胞型。肿瘤细胞排列成管状、索样、鹿角样，伴显著的纤维间质（A，D）。肿瘤条索与非肿瘤性肝细胞索以替代生长的方式相连续（G）。肿瘤细胞无粘液分泌（B），角蛋白 7（E）和 19（H）常阳性，KIT（C），NCAM1/CD56（F）和 EpCAM（I）呈强弱不等的阳性。

CLC

- 罕见，占原发肝癌1%
- 来源于小胆管或赫令氏管（肝脏祖细胞起源）
- 胆管反应样、吻合腺体，大量丰富纤维间质中
- 交界性潜能

Clinicopathological study on cholangiolocellular carcinoma suggesting hepatic progenitor cell origin. Hepatology. 2008;47:1544–1556.

- 灰白、实性、小叶状、无包膜，边界不规则
- 小而一致腺体、鹿角样吻合
- 丰富透明变性和/或水肿纤维性间质
- 细胞立方（＜肝细胞）、缺乏嗜酸性胞浆
  核圆、核仁明显
- 无黏液产生、无出血坏死
- 表达CK19、 CK7、NCAM、EpCAM
- HEP、CD10阴性

A

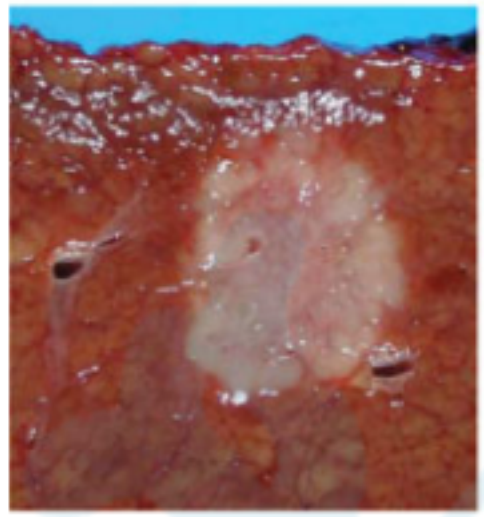

B

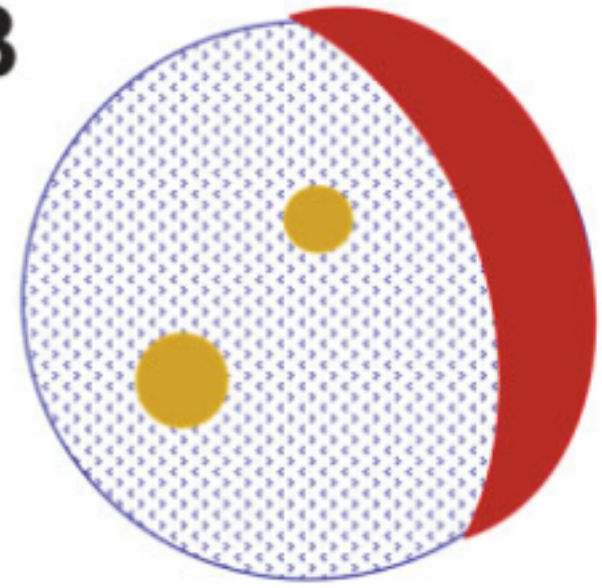

CC

CLC

HCC-like area

C

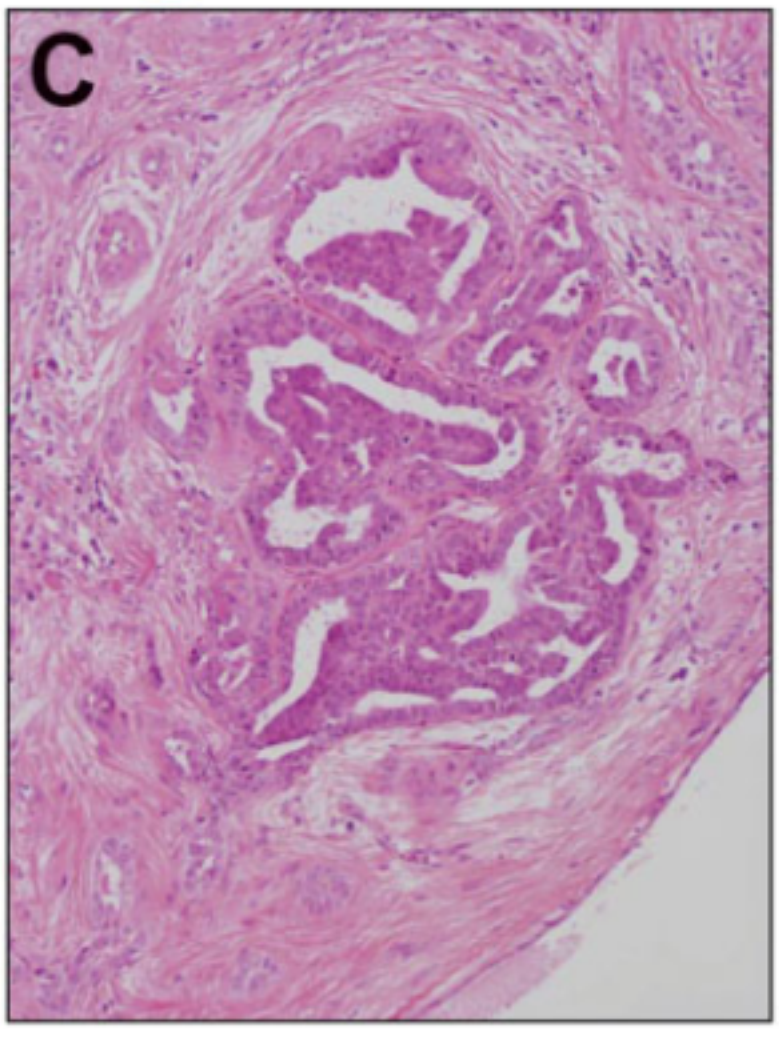

D

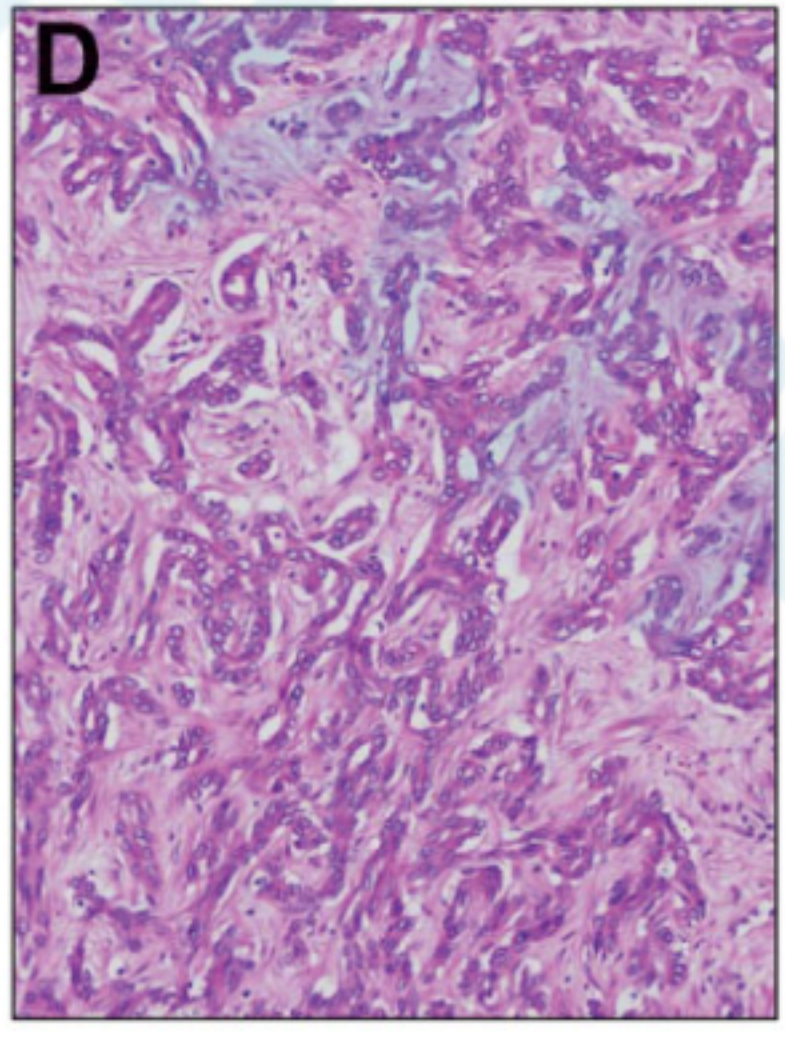

E

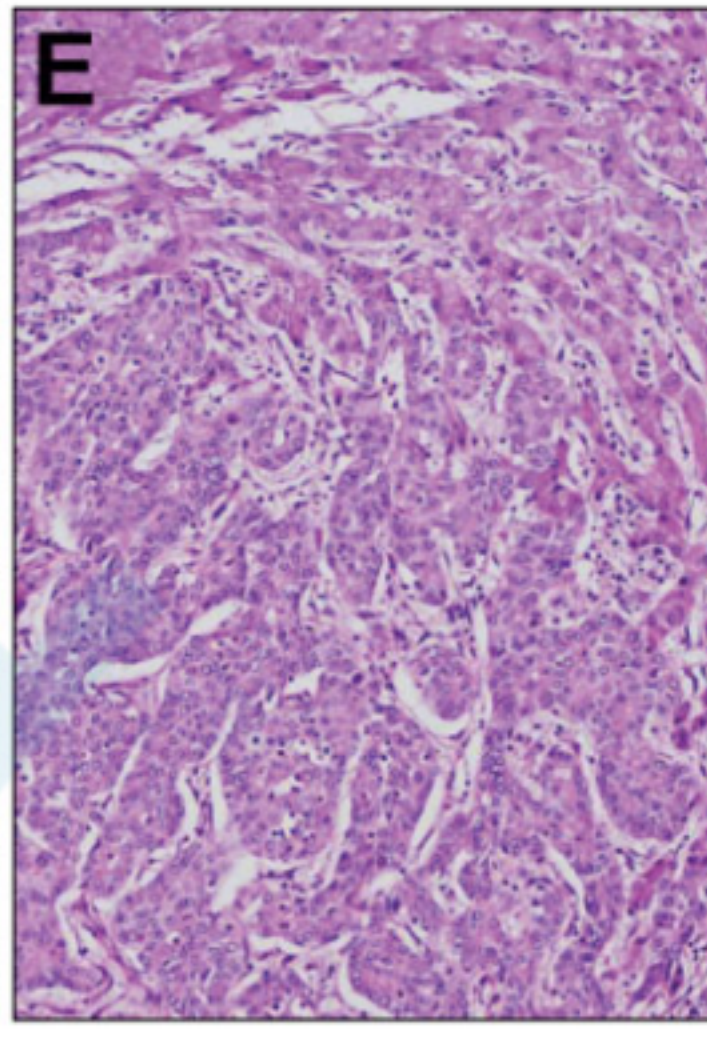

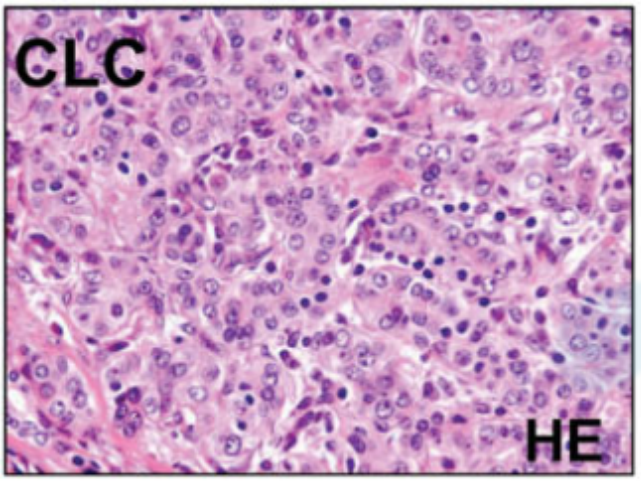
CLC
HE

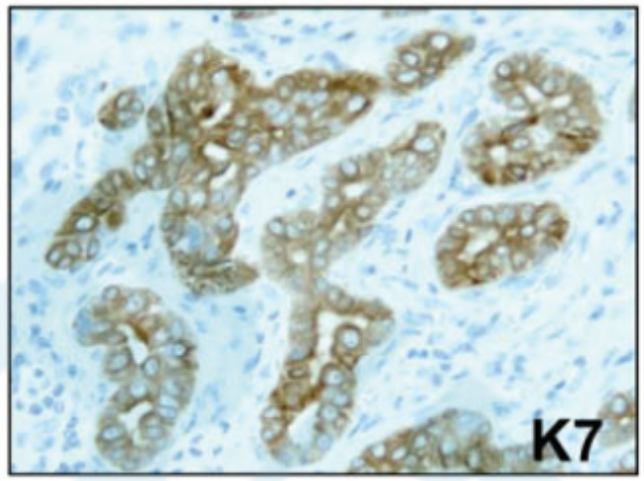
K7

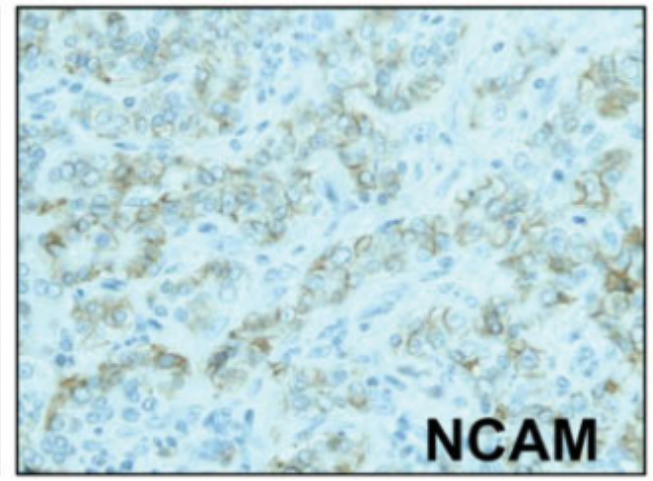
NCAM

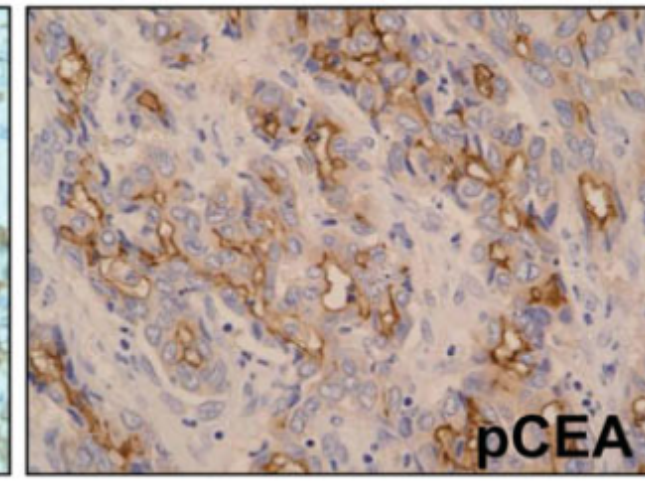
pCEA

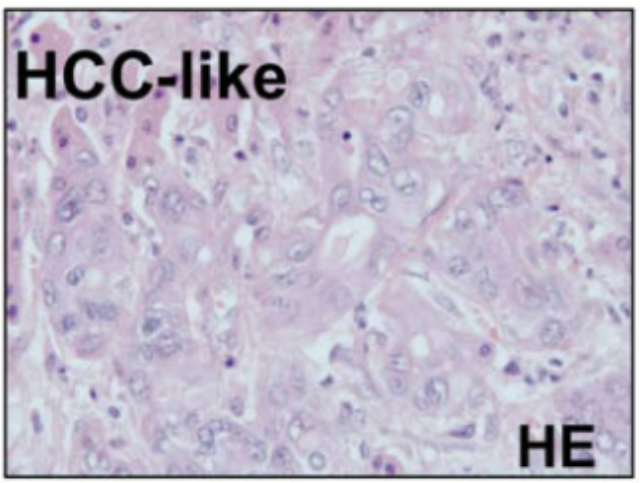
HCC-like
HE

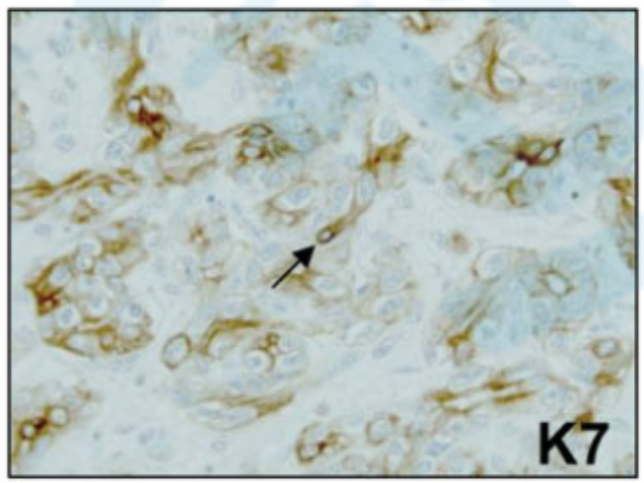
K7

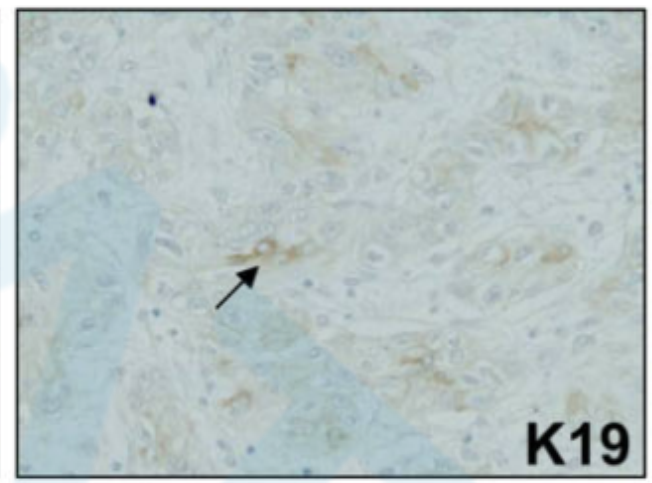
K19

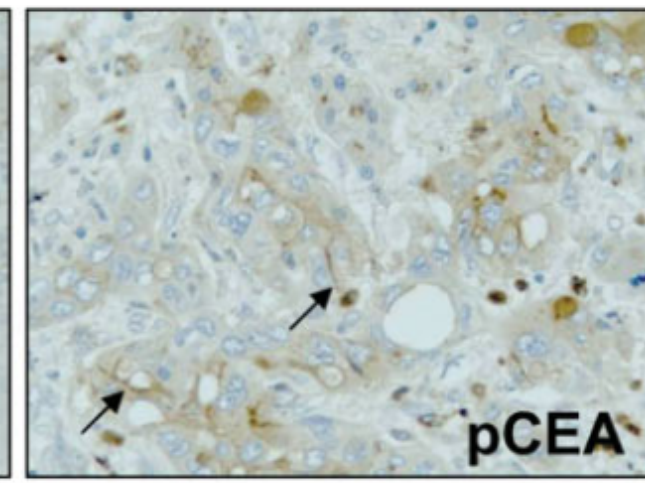
pCEA

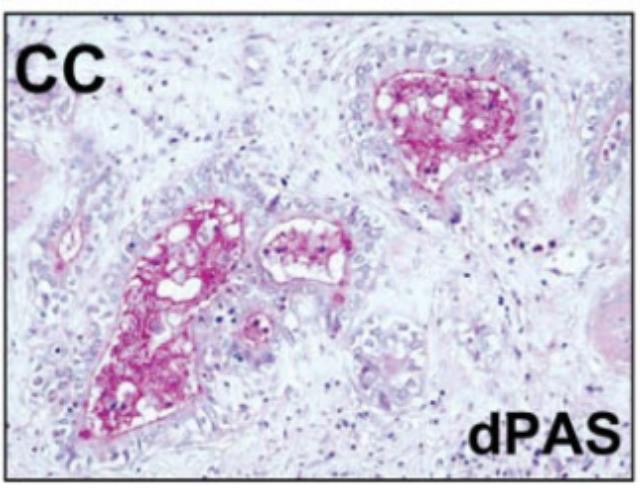
CC
dPAS

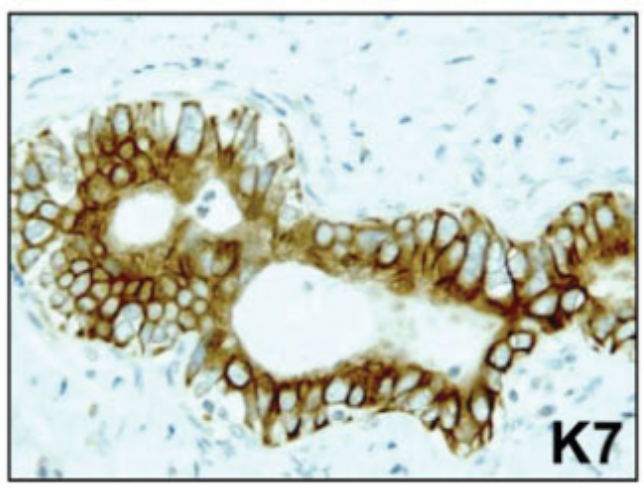
K7

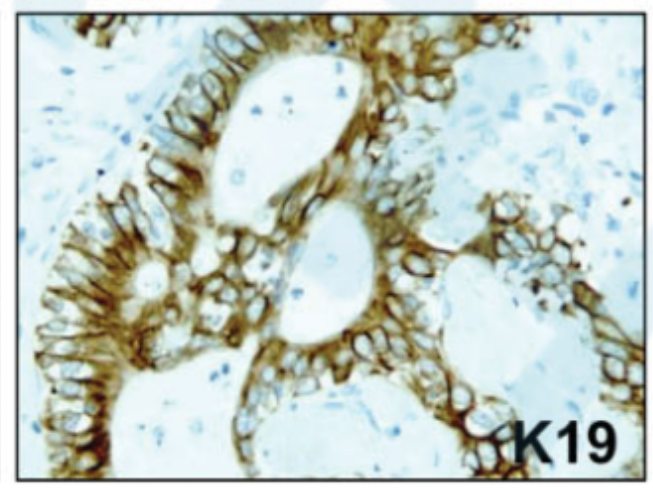
K19

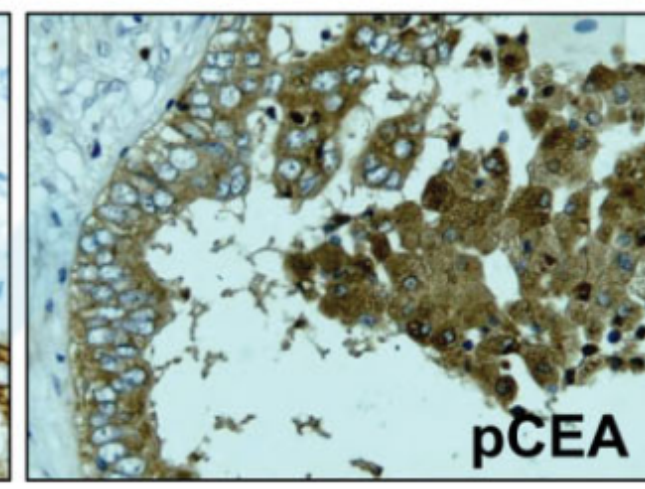
pCEA

ductal plate malformation (DPM)

- 导管盘：胎儿肝的独特结构
- 伴随肝内胆管重塑逐渐消失（出生后）
- 见于纤维囊性疾病：先天性肝纤维化、Caroli病， von Meyenburg 复合体

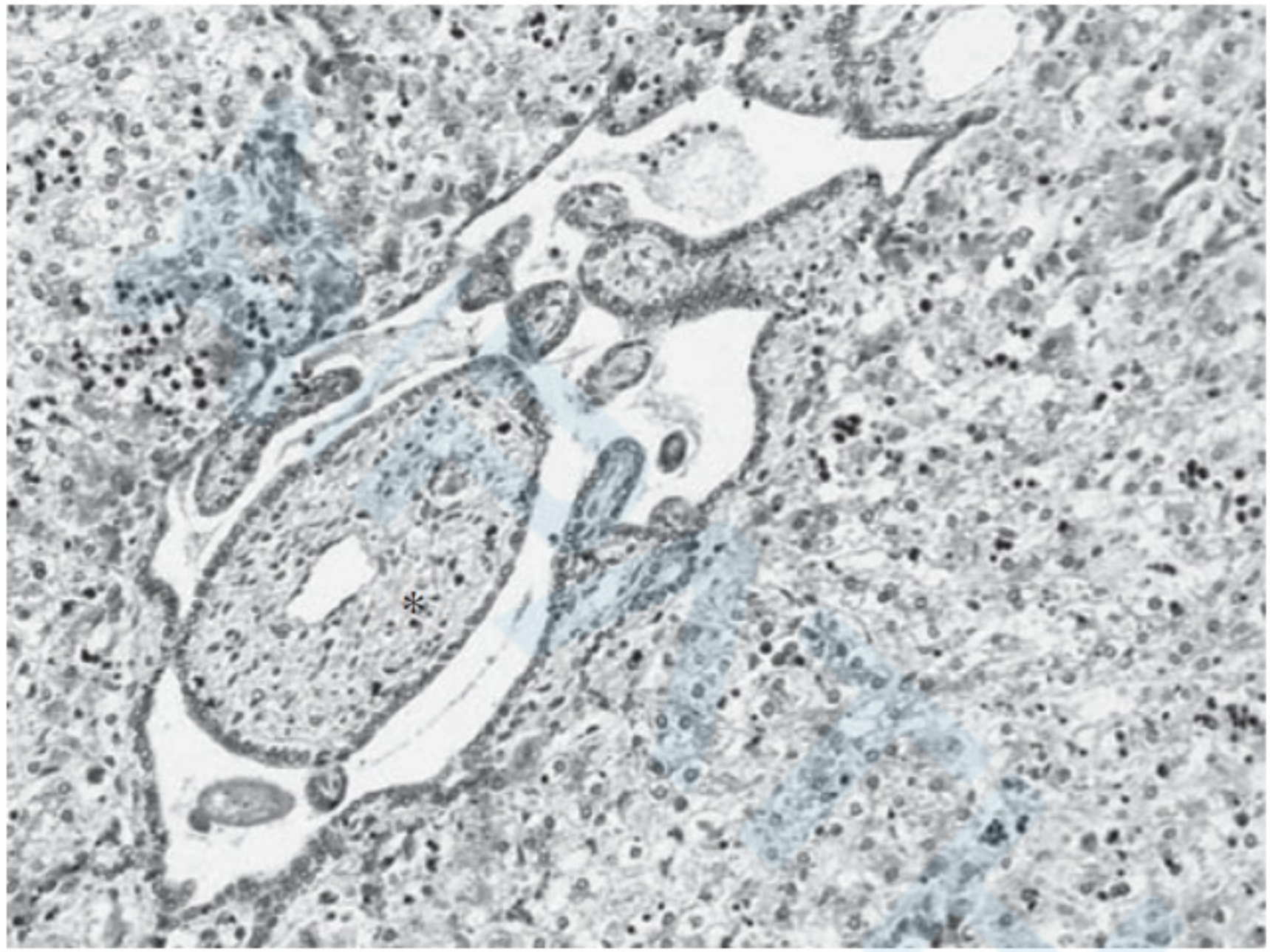

FIGURE 1. Ductal plate malformation in congenital hepatic fibrosis. Duct structures in the periportal area are irregularly dilated, with some showing bridging, and some part of portal tract (*) is surrounded by dilated ducts (HE).

CCA伴DPM模式—新亚型

- 10例分化很好腺癌，易与DPM混淆
- 腺体不规则扩大，内衬单层立方、矮柱状细胞伴不规则凸起，类似DPM
- 边缘替代肝小叶，中心纤维间质及较少细胞
- 表达CK19、 EMA腔面， HEP、MUCIN阴性
- Ki67<10% P53几乎不表达
- 预后较CCA 好

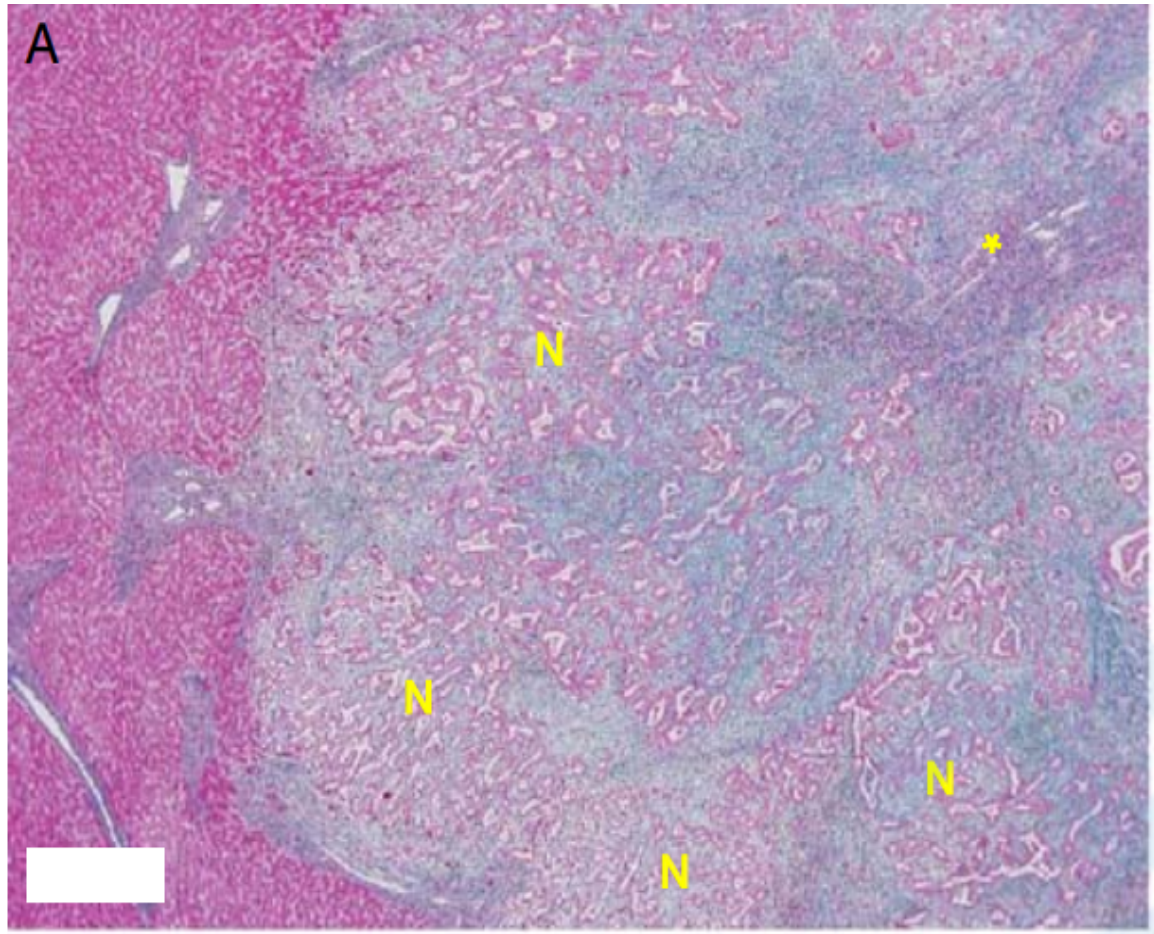
A
N
N
N
N
*

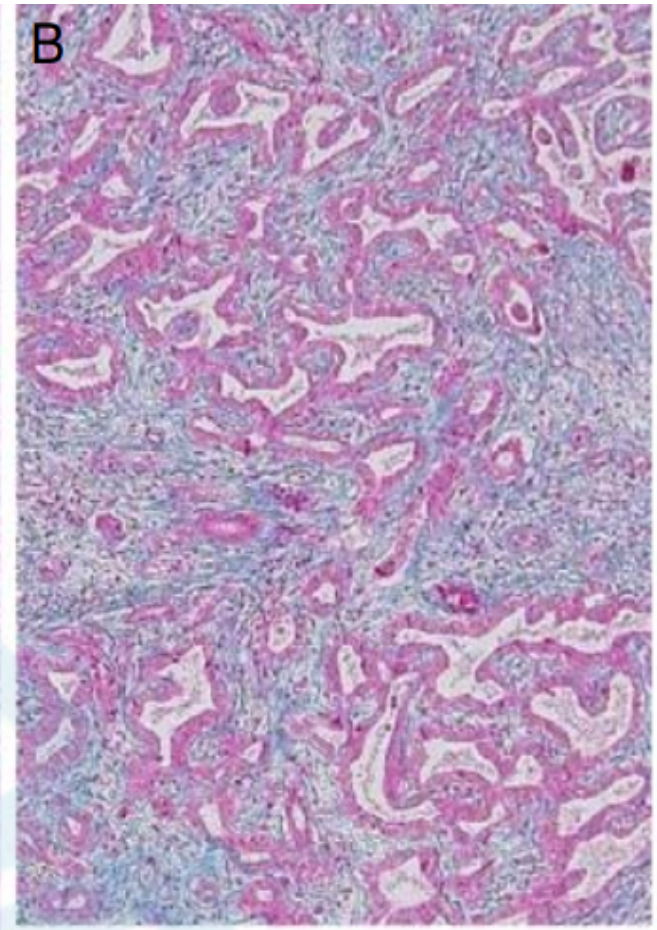
B

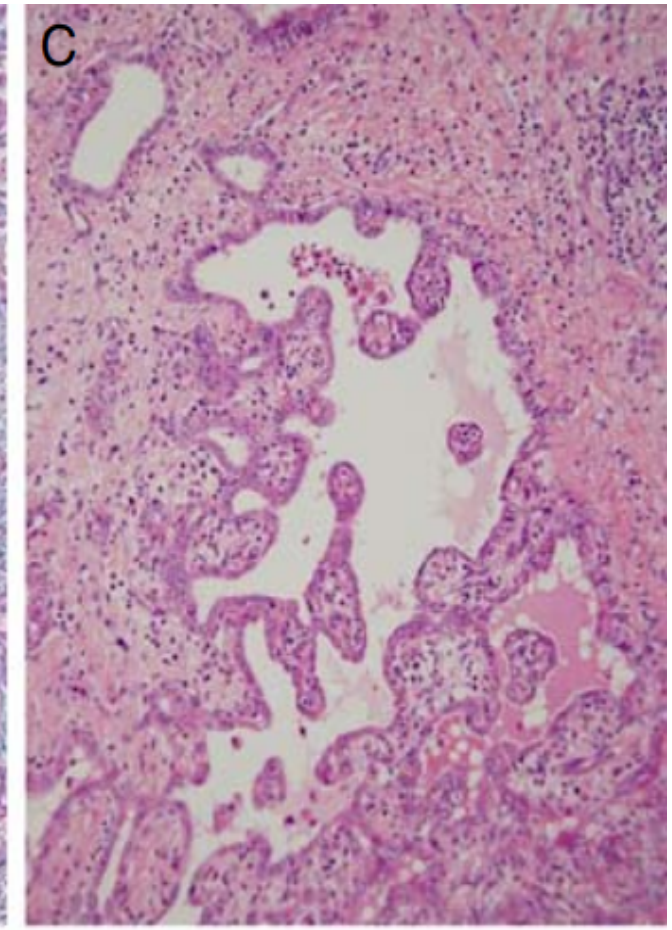
C

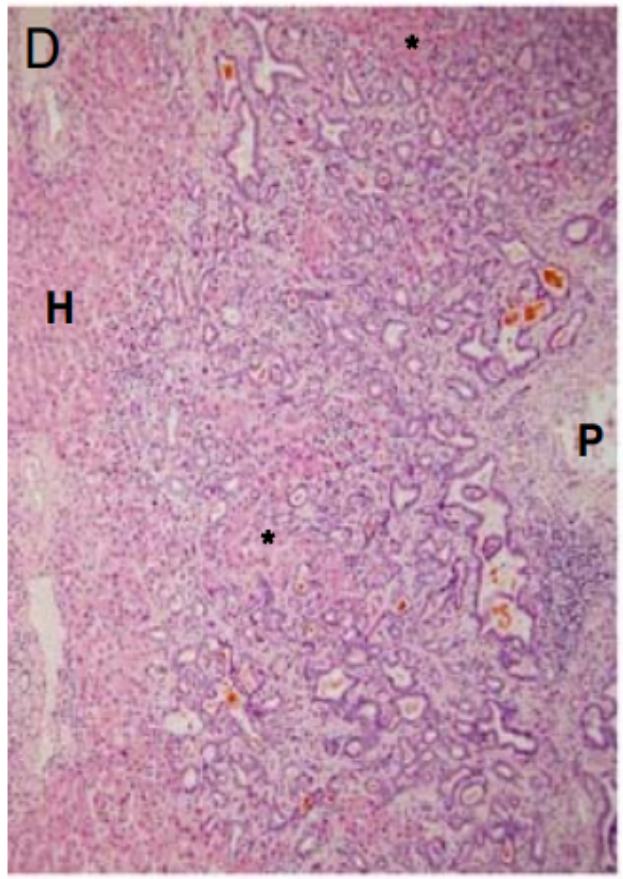
D
H
P
*
*

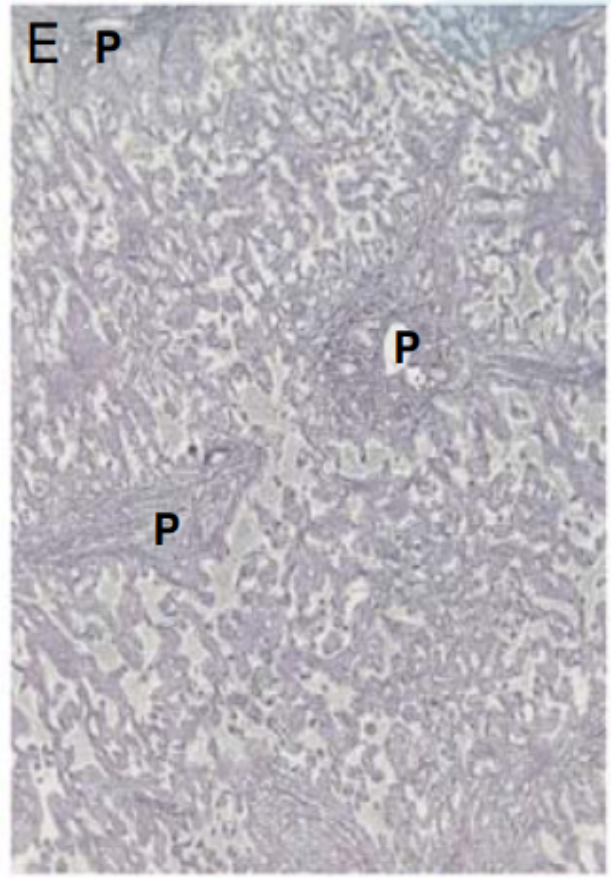
E
P
P
P

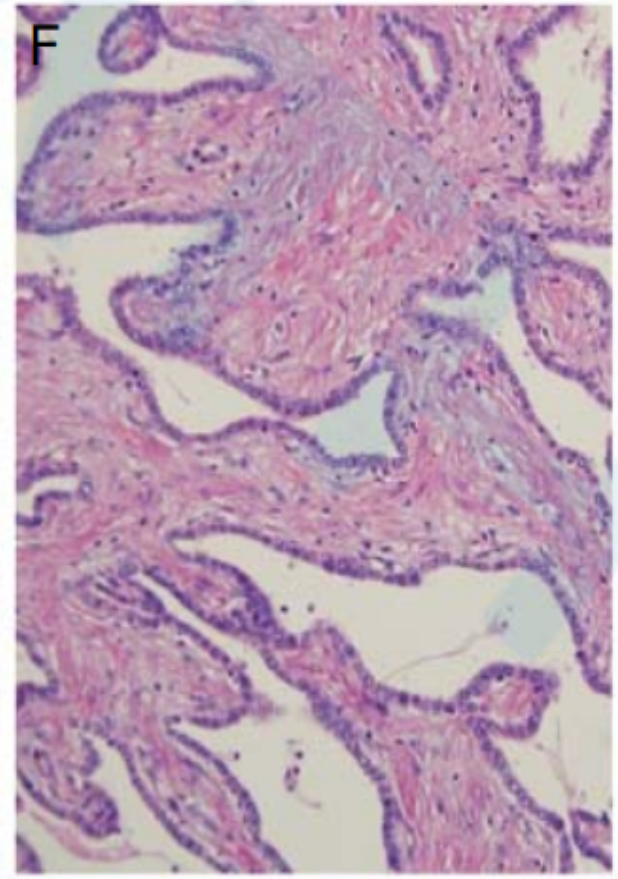
F

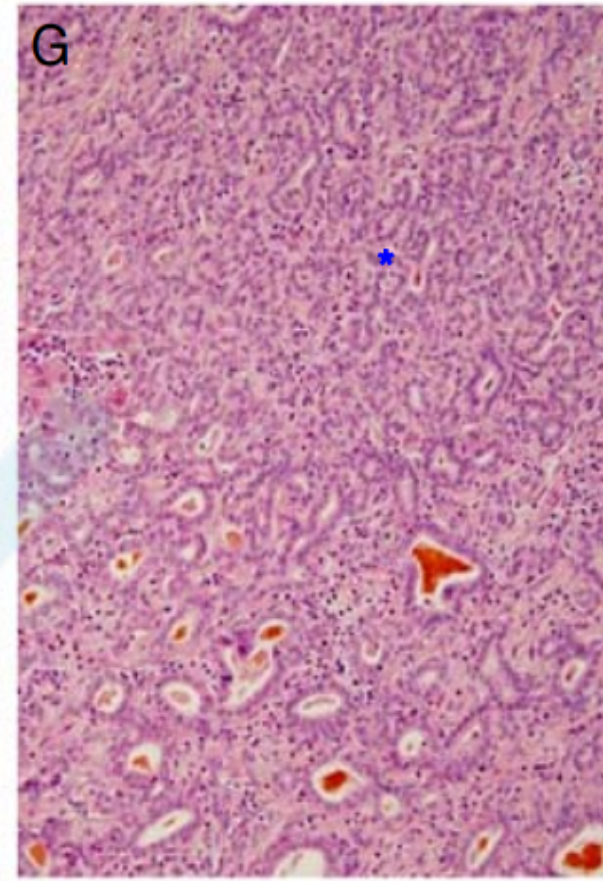
G
*

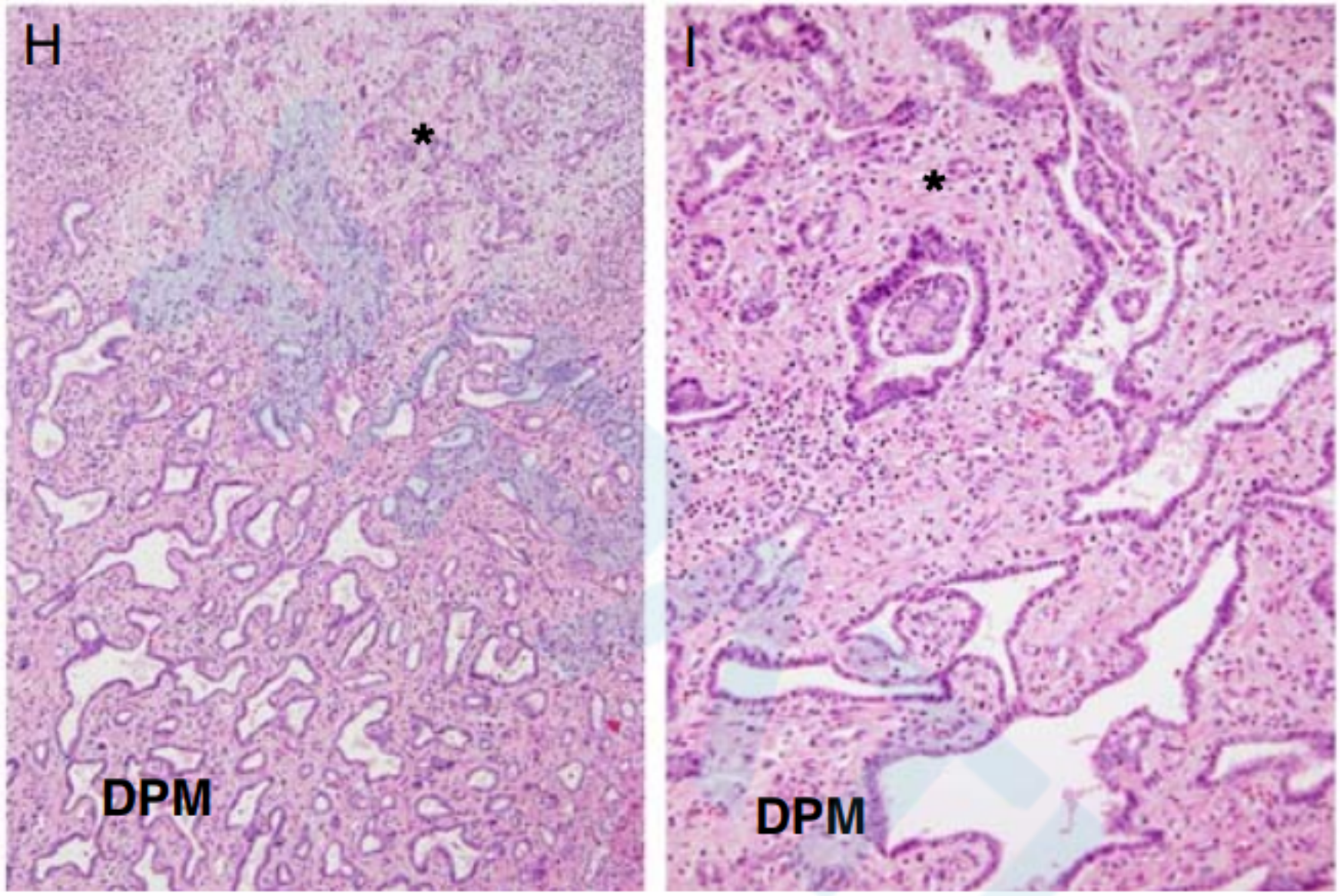

Intrahepatic cholangiocarcinoma with predominant “ductal plate malformation” pattern: a new subtype. Am J Surg Pathol. 2012;36:1629–1635.

背景

- HCC、CCA基因改变及临床病例特征研究有进展
- HCC--TERT, CTNNB1, TP53,ARID2, ARID1A, and AXIN1
- CCA--TP53 ,KRAS, SMAD4, IDH1/2, ARID1A, BAP1, and PTEN

背景

- 关于胆道特征的cHCC-CCA及CLC的研究局限
- 罕见、复杂、组织病理分类多
- 尤其是基因改变-组织学特征关联（分子-形态）
- 作者认为cHCC-CCA及CLC基因改变与组织学特征应该有关

目 的

- 原发性肝癌中基因改变-组织学特征联系
- 重点：CLC成份及DPM模式与基因改变关系

材料与方法

- 77例cHCC-CCA及CLC（1996-2017）
- 女22例，男55例
- 年龄36-83（平均65.8岁）
- 外科切除标本
- 常规HE、网染、黏液染色
- IHC
- 分子检测： KRAS, IDH1, IDH2，hTERT

TABLE 2. Primary Antibodies Used

Primary Antibody	Type (Clone)	Pretreatment	Dilution	Source
ARID1A	Rabbit polyclonal	eARI-BA (121°C, 5 min)	1:300	Sigma, St. Lois, MO
ARID2	Mouse mono (E-3)	eARI-BA (121°C, 5 min)	1:300	Santa-Cruz, Santa-Cruz, CA
BAP1	Mouse mono (C-4)	eARI-BA (121°C, 5 min)	1:100	Santa-Cruz
PBRM1	Rabbit polyclonal	eARI-BA (121°C, 5 min)	1:200	Bethyl, Montgomery, TX
p53	Mouse mono (DO7)	MW-CB (95°C, 20 min)	1:100	Dako Carpinteria, CA
CK7	Mouse mono (OV-TL 12/30)	MW-CB (95°C, 20 min)	1:50	Dako
CK19	Mouse mono (RCK108)	MW-CB (95°C, 20 min)	1:100	Dako
EMA	Mouse mono (E29)	MW-CB (95°C, 20 min)	1:200	Dako
MUC1	Mouse mono (DF3)	MW-CB (95°C, 20 min)	1:50	Dako
EpCAM	Mouse mono (HEA125)	MW-CB (95°C, 20 min)	1:5	Abcam, Cambridge, UK
NCAM/CD56	Mouse mono (1B6)	MW-CB (95°C, 20 min)	Prediluted	Nichirei, Tokyo, Japan
AFP	Rabbit polyclonal	MW-CB (95°C, 20 min)	1:500	Dako
HepPar1	Mouse mono (OCH1E5)	MW-CB (95°C, 20 min)	1:100	Dako

AFP indicates alpha-fetoprotein; ARID1A, AT-rich interactive domain-containing protein 1A; BA, 0.05 M boric acid buffer (pH 8); BAP1, BRCA1-associated protein-1; CB, 0.05 M citric acid buffer (pH 6); CK, cytokeratin; eARI, electronic antigen retrieval instrument; EMA, epithelial membrane antigen; EpCAM, epithelial cell adhesion molecule; MW, microwave; NCAM, neural cell adhesion molecule; PBRM1, protein polybromo-1.

ARIDIA、PBRMB1、ARID2、BAP1

- SWI/SNF染色质重塑复合物亚基（15个）
- SWI/SNF染色质重塑复合物 存在于所有真核细胞中
- 调节细胞发育、分化、增殖、DNA修复及肿瘤抑制功能
- 与基因转录激活及抑制有关
- 肿瘤发生发挥重要作用
- 表达缺失提示基因突变

TABLE 1. Histologic Subgroups Based on the Proportion of CLC

Group	Definition	No. Patients
Group A	CLC-predominant: CLC (+CCA) component > 80% of the tumor	29
A1	CLC with CCA (cCLC-CCA)	5
A2	Pure CLC (classic CLC)	11
A3	CLC with focal HCC and/or INT (cHCC-CLC, cINT-CLC)	13
Group B	With CLC: CLC (+CCA) component, 5%-80% of the tumor	31
B1	CLC with HCC and/or INT (cHCC-CLC, cINT-CLC)	11
B2	Classical type cHCC-CCA (cHCC-CCA)	9
B3	HCC and/or INT with focal CLC (cHCC-CLC, cINT-CLC)	11
Group C	Without CLC: CLC (+CCA) component, <5% of the tumor (INT)	17

DPM

DPM 按程度分为3组

- 0 无 （<5%） 40
- 1 局部（5-50%）18
- 2 大量（>50） 19

结果

TABLE 3. The Association of Histologic Subgroups Based on Proportion of CLC With Clinicopathologic Features

	A (n = 29)	A1 (n = 5)	A2 (n = 11)	A3 (n = 13)	B (n = 31)	B1 (n = 11)	B2 (n = 9)	B3 (n = 11)	C (n = 17)	*P*
Age (y)										< 0.05, A2 vs. C
Mean	67.2	68.0	70.3	64.5	66.4	65.1	68.9	65.6	62.1	
Range	44-81	59-74	52-83	44-81	52-78	52-73	58-78	56-75	36-77	
Sex (male %)	86.2	80	100	76.9	66.4	63.6	55.6	63.6	64.7	< 0.05, A vs. B
M/F	25/4	4/1	11/0	10/3	19/12	7/4	5/4	7/4	11/6	
Etiology										NS
B	4	0	1	3	9	1	4	4	3	
C	8	1	3	4	13	7	3	3	7	
Alcohol	3	0	2	1	2	0	0	2	1	
NAFLD	4	0	1	3	4	3	1	0	0	
Others/unknown	10	4	4	2	3	0	1	2	6	
Virus (B or C)										< 0.05, A vs. B
+	12	1	4	7	22	8	7	7	10	
−	17	4	7	6	9	3	2	4	7	
Stage										NS
1	4	1	2	1	5	0	1	4	1	
2	9	0	4	5	15	8	5	2	8	
3	11	1	4	6	3	1	1	1	3	
4	5	3	1	1	8	2	2	4	5	
Lymph node metastasis										NS
+	1	0	1	0	2	0	0	2	3	
−	28	5	10	13	29	11	9	9	14	
Metastasis										NS
+	3	2	0	1	4	2	1	1	0	
−	26	3	11	12	27	9	8	10	17	

TABLE 3. The Association of Histologic Subgroups Based on Proportion of CLC With Clinicopathologic Features

	A (n = 29)	A1 (n = 5)	A2 (n = 11)	A3 (n = 13)	B (n = 31)	B1 (n = 11)	B2 (n = 9)	B3 (n = 11)	C (n = 17)	*P*
Metastasis										NS
+	3	2	0	1	4	2	1	1	0	
−	26	3	11	12	27	9	8	10	17	
Tumor size (mm)										<0.05; C vs. A, B
Mean	3.8	6.4	2.9	3.5	3.7	4.1	4.1	2.9	5.8	
Range	1.0-13	1.8-13	1.5-5.3	1.0-7.3	0.5-16	1.7-16	0.6-8.5	0.5-5.5	2.0-13	
Vp/im										NS
+	18	4	4	10	22	6	7	9	15	
−	11	1	7	3	9	5	2	2	2	
AFP										NS
+	8	1	2	5	12	3	4	5	6	
−	21	4	9	8	19	8	5	6	11	
Previous therapy										<0.05; A vs. B
+	2	0	0	2	10	4	3	3	4	
−	27	5	11	11	21	7	6	8	13	
Multiple tumors										<0.01; B vs. A, C
+	5	1	1	3	16	5	5	6	1	
−	24	4	10	10	15	6	4	5	16	
DPM-pattern										<0.01; A vs. B, C
0	3	1	0	2	23	8	7	8	17	<0.05; B vs. C
1	11	1	4	6	6	1	2	3	0	
2	15	3	7	5	2	2	0	0	0	
Diversity score										<0.01; B vs. A, C
1-2	20	4	11	5	8	4	0	4	13	
3-5	9	1	0	8	23	7	9	7	4	
Fibrosis										<0.01; A1-A2 vs. B
0	5	3	2	0	1	1	0	0	3	
F1,2	6	1	4	1	6	1	3	2	3	
F3,4	18	1	5	12	24	9	6	9	11	

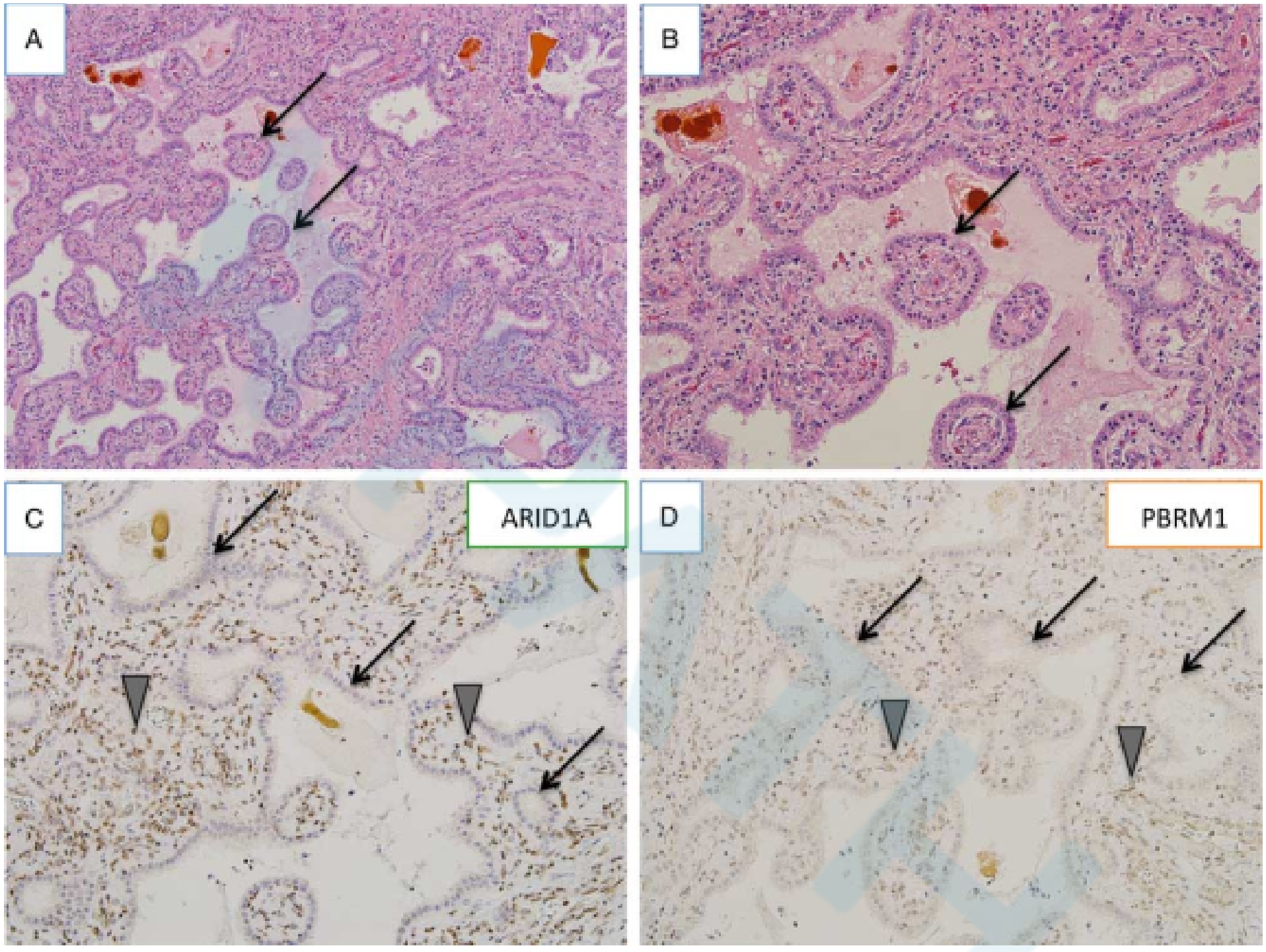

FIGURE 1. Representative histology of DPM-pattern and immunohistochemical detection of *ARID1A* and *PBRM1* alterations. A and B, Carcinoma cells form irregularly dilated and anastomosing tubular structures with fibrous core (arrows). A 76-year-old male, subgroup A-2, nonalcoholic fatty liver disease, F4. Hematoxylin and eosin. C and D, Carcinoma cells do not show immunoreactivity for ARID1A and PBRM1 (arrows), whereas background inflammatory and stromal cells are positive (arrowheads). Immunostaining for ARID1A and PBRM1 counterstained by hematoxylin.

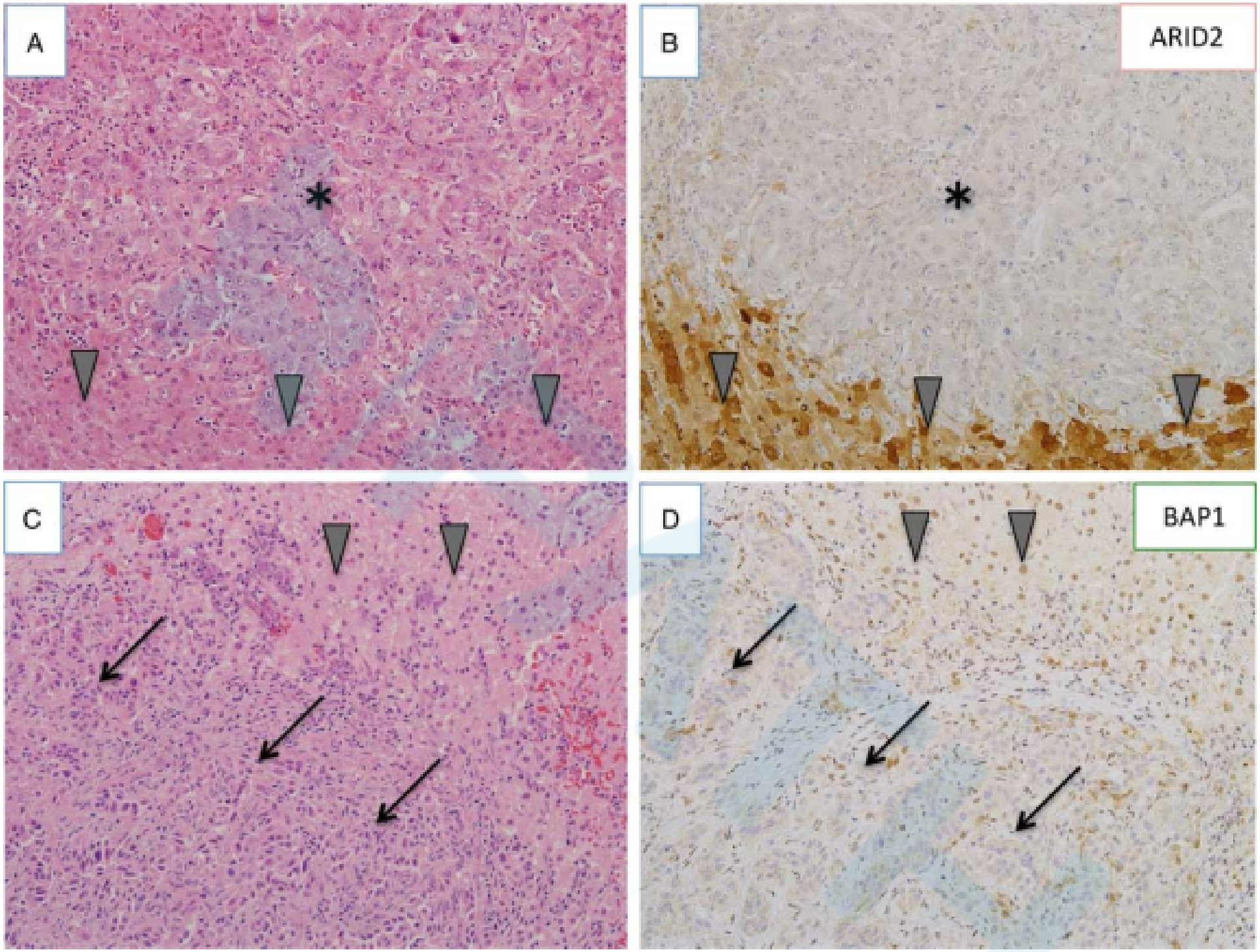

FIGURE 2. Representative immunohistochemical detection of *ARID2* and *BAP1* alterations. A and B, Carcinoma cells resembling hepatocytes (asterisk) do not show immunoreactivity for ARID2, whereas background hepatocytes are positive (arrowheads). A 64-year-old male, group C, HCV-positive, F4. C and D, Carcinoma cells showing trabecular pattern (arrows) do not show immunoreactivity for BAP1, whereas background hepatocytes are positive (arrowheads). A 71-year-old male, group C, HCV positive, F4. Hematoxylin and eosin (A and C) and immunostaining for ARID2 (B) or BAP1 (D) and hematoxylin.

TABLE 4. The Association of Histologic Subgroups Based on Proportion of CLC With Genetic Alterations

	Total (n = 77)	A n = 29)	A1 (n = 5)	A2 (n = 11)	A3 (n = 13)	B (n = 31)	B1 (n = 11)	B2 (n = 9)	B3 (n = 11)	C (n = 17)	
hTERT (n [%])	19 (24.7)	2 (6.9)	0	0	2 (15.4)	12 (38.7)	4 (36.4)	3 (33.3)	5 (45.5)	5 (29.4)	$P < 0.01$; A vs. B $P < 0.05$; A vs. C
ARID1A (n [%])	16 (20.8)	12 (41.4)	2 (40)	6 (55)	4 (30.8)	3 (9.7)	1 (9.1)	0	2 (18.2)	1 (5.9)	$P < 0.01$; A vs. B $P < 0.05$; A vs. C
PBRM1 (n [%])	15 (19.5)	4 (13.8)	0	0	4 (30.8)	6 (19.4)	4 (36.4)	0	2 (18.2)	5 (29.4)	$P < 0.01$; A1+A2 vs. A3+B1, C $P < 0.05$; B2 vs. A3+B1, C
ARID2 (n [%])	2 (2.6)	0	0	0	0	1 (3.2)	1 (9.1)	0	0	1 (5.9)	NS
BAP1 (n [%])	1 (1.3)	0	0	0	0	0	0	0	0	1 (5.9)	NS
p53 (n [%])	35 (45.5)	10 (34.5)	2 (40)	3 (27)	5 (38.5)	19 (61.3)	7 (63.6)	6 (66.7)	6 (54.5)	6 (35.3)	$P < 0.05$ A vs. B
KRAS (n [%])	4 (5.2)	1 (3.4)	0	0	1 (7.7)	3 (9.7)	0	2 (22.2)	1 (9.1)	0	NS
IDH1/2 (n [%])	6 (7.8)	2 (6.9)	0	2 (18)	0	3 (9.7)	0	1 (11.1)	2 (18.2)	1 (5.9)	NS
Any alterations (n [%])	64 (83.1)	23 (79.3)	4 (80)	9 (82)	10 (77)	27 (87)	10 (91)	9 (100)	8 (73)	14 (82)	NS
No. alterations											NS
0	13	6	1	2	3	4	1	0	3	3	
1	41	16	4	7	5	15	5	7	3	10	
2	15	6	0	2	4	6	3	1	2	3	
3	6	1	0	0	1	4	2	1	1	1	
4	2	0	0	0	0	2	0	0	2	0	
No. SWI/SNF alterations											$P < 0.05$, B2 vs. A2, A3, B1
0	49	3	3	5	8	22	6	9	7	11	
1	22	2	2	6	2	8	4	0	4	4	
2	6	0	0	0	3	1	1	0	0	2	

NS indicates nonsignificant.

结果

- hTERT启动子突变（24.7%）A组较B、C组少见
- ARIDIA改变（20.8%） A组较B、C组多见
- PBRM1改变（19.5%）A3、B1组较A1、A2组多
  C组较A1、A2及B2组多
- ARID2改变（2.6%）2例（B1、C组）
- BAP1（1.3%）1例（C组）
- P53（45.5%）A组较B组少

- 各组基因改变数量无差异
- B2组无SWI/SNF组（ARID1A、ARID2、PBRM1）改变
- A2、A3、B1组更多SWI/SNF基因改变

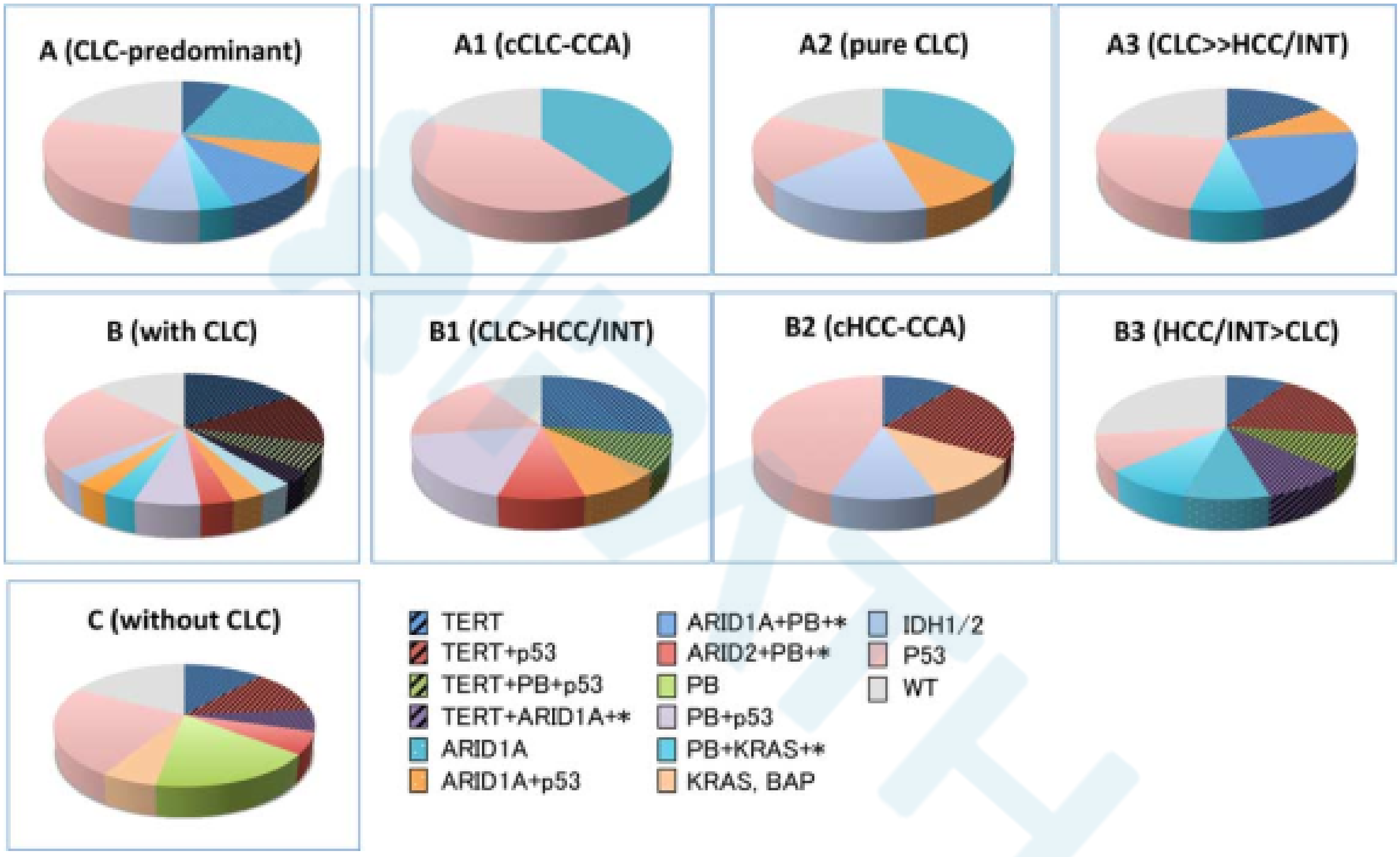

FIGURE 3. Pie chart representation of the genetic alterations in each histologic subgroup. *Other genes.

A组ARIDIA及P53是主要基因改变
B组主要是hTERT突变伴或不伴p53、PBRM1及ARIDIA突变

TABLE 5. Association of DPM-Pattern and Genetic Alterations

	DPM-Pattern			
	Extensive	**Focal**	**Absent**	***P***
hTERT mut (19)	0	3	16	< 0.01
WT (58)	19	15	24	
ARIDIA mut (16)	11	3	2	< 0.01
WT (61)	8	15	38	
PBRMI mut (15)	4	1	10	NS
WT (62)	15	17	30	
BAPI mut (1)	0	0	1	NS
WT (76)	19	18	39	
ARID2 mut (2)	0	0	2	NS
WT (75)	19	18	38	
p53 mut (35)	6	9	20	NS
WT (42)	13	9	20	
KRAS mut (4)	0	2	2	NS
WT (73)	19	16	38	
IDHI2 mut (6)	2	1	3	NS
WT (71)	17	17	37	

NS indicates nonsignificant.

ARID1A突变与DPM程度正相关
hTERT启动子突变与DPM负相关

讨 论

- 迄今最大量研究数据
- CLC为主者组ARID1A频繁突变
  hTERT突变罕见

讨 论

- 首次发现ARID1A改变与DPM模式密切相关
- ARID1A改变与CLC及DPM可同时出现
- ARID1A改变可能具有CLC伴DPM特征
- CLC伴DPM可能代表ARID1A基因失活引起的异常分化

讨 论

- ARID1A可帮助鉴别良恶性DPM模式
- 本文中7例中16个 Von Meyenburg 复合体均无缺失表达
- DPM模式类似于胆道良性疾病，有时与LCL相关
- hTERT突变在伴有DPM中发生少

讨 论

- 首次证明PBRM1突变是cHCC-CCA及CLC常有的基因改变
- BAP1及ARID2改变罕见

讨 论

- B2组没有SWI/SNF组（ARID1A、ARID2、PBRM1）改变
- 经典型cHCC-CCA
- 独特致癌作用与SWI/SNF改变无关
- P53突变率最高

小结

- CLC独特亚型，可与HCC、CCA及cHCC-CCA混合
- CLC为主组年龄较大、男性为主及体积较小为特征
- ARID1A基因改变在CLC为主组最多，且与DPM程度相关
- hTERT及P53相对较少在CLC为主组

小结

- 建议原发性肝癌应统一术语
- CLC主要成分组与CHCC-CAA不同基因改变及临床病理特征
- 独特组织学亚型区别于cHCC-CCA
- ARID1A改变可能是CLC伴DPM的特征
- 可作为诊断有用标记

谢 谢